Growth hormone induces TGF-β1 in podocytes: Implications in podocytopathy and proteinuria

Dhanunjay Mukhi[1], Rajkishor Nishad[1], Ram KumarMenon[2], Anil KumarPasupulati[1]*

[1]Department of Biochemistry, School of Life Sciences, University of Hyderabad, Hyderabad, India-500046,

[2]Departments of Pediatrics and Molecular & Integrative Physiology, University of Michigan, Ann Arbor, USA-48109.

Running title: GH induces TGF- β1 in podocytes

Correspondence to:

Anil Kumar Pasupulati, School of Life Sciences, University of Hyderabad, Gachibowli, Hyderabad, India. Tel: +91-040-23134519; Email: pasupulati.anilkumar@gmail.com

Keywords: Growth hormone; podocytes; proteinuria; TGF-β; SMADs.

Abstract:

GH had direct effects on the glomerular podocytes. Increased levels of GH are implicated in the pathogenesis of renal abnormalities in acromegaly and diabetic nephropathy (DN) in Type 1 diabetes mellitus. We investigated the role of TGF-β1 in GH's effects on the glomerular podocytes. Exposure of podocytes to GH resulted in elevated expression of TGF-β1 and is concurrent with increased phosphorylation of SMAD2/3 and accumulation of SMAD4. Conditioned media from podocytes exposed to GH also triggered TGF-β1 and activated SMAD signaling. GH and conditioned medium from GH-treated cells altered podocyte permeability. GH induced podocyte hypertrophy *in vitro* concurrently mice injected with GH demonstrated increased kidney size, glomerular enlargement, podocyte hypertrophy, and proteinuria. Renal manifestations in GH injected mice were associated with increased TGF-β1 expression and activation of TGF-β1 signaling. Administration TGF-β receptor antagonist (SB431542) prevented GH induced renal manifestations and proteinuria. Diabetic mice devoid of the GH receptor in podocytes ($pGHR^{-/-}$) are protected from glomerular hypertrophy and sclerosis. Blunting GH/GHR axis in diabetic settings improved proteinuria. These results provide a novel mechanistic link between GH and glomerular dysfunction in clinical conditions such as diabetes and acromegaly and are mediated via TGF-β expression.

Introduction:

Diabetic nephropathy (DN) is characterized by an array of structural and functional aberrations in the nephron. Structural changes include podocyte hypertrophy, glomerular sclerosis, and thickening of glomerular basement membrane (GBM). The functional manifestations include a short-time increase in glomerular filtration rate (GFR), proteinuria ranging from microalbuminuria to overt proteinuria. The magnitude of proteinuria dictates the extent of damage to the glomerular filtration barrier (GFB), which consists of endothelial cells, basement membrane, and podocytes [1]. Podocytes are the specialized cells that provide epithelial coverage to renal capillaries and serves as a final barrier to curb protein loss into urine. Injury to the podocytes including hypertrophy, foot process effacement, and epithelial-mesenchymal-transition (EMT) results in reduced podocyte count [2]. Podocyte loss leaves GBM denuded and provokes neighboring podocytes to undergo compensatory hypertrophy. However, the molecular signals that initiate the podocyte or glomerular hypertrophy remains unclear.

Elevated growth hormone (GH) levels in poorly controlled type 1 diabetes mellitus (DM) is implicated as a causative factor in the development of renal aberrations and proteinuria [2-4]. GH transgenic animals developed significant renal hypertrophy and glomerulosclerosis [5]. Albeit, part of the biological effects of GH are mediated by insulin-like growth factor 1 (IGF-1), the glomerular hypertrophy and significant renal manifestations are evidenced in GH transgenics with IGF-1 null background suggesting that GH, but not IGF-1 responsible for glomerular hypertrophy [6]. In GH transgenic animals, podocytes undergo hypertrophy while mesangial and endothelial cells undergo proliferation [6]. GH administration pronounced the usual renal hypertrophy and it was aggravated in streptozotocin (STZ)-induced diabetic rats [5]. Mice with mutant GHR were protected from STZ-induced diabetic renal complications [7].

Similarly, somatostatin analogs (lanreotide and octreotide) offered substantial protection against the DN [8]. Long-term treatment of acromegaly patients with somatostatin analogues prevented the GH-induced renal manifestations [9]. This evidence argues a strong association between elevated GH levels and renal biology. Our earlier studies identified that podocyte is a direct target for GH action and our subsequent studies demonstrated that GH regulates expression of smad interacting protein (SIP1) and transforming growth factor β interacting protein (TGFBIP, also known as Big-h3) in podocytes [10-12].

TGF-β is a master regulator of ECM turnover that is secreted from most of the cell types in the body. Among three isoform, TGF-β1 has been associated with pathophysiology of DN. Earlier studies suggest that TGF-β1 is implicated as a central molecule responsible for the excess deposition of ECM proteins during diabetes [13]. Both mRNA and protein levels of TGF-β1 are significantly elevated in DN patients [14, 15]. Studies from experimental diabetic animals further substantiated the role of TGF-β1 in the pathogenesis of DN [16]. Neutralizing antibodies against TGF-β1 reversed the type II diabetic renal injury [17]. In continuation to the existing studies, here we show that supraphysiological doses of GH induce renal hypertrophy and proteinuria that involves the activation of TGF-β/SMAD pathway. Furthermore, employing immortalized human podocytes we studied how GH imposes functional impairment in podocytes. Our studies also demonstrated that inhibitor for TGF-βR1 (SB431542) prevents early features of DN.

Materials and methods:

Materials: TGF-β1 antibody (#MA5-16949) and Lipofectamine (#11668019) were purchased from Invitrogen. SMAD pathway antibodies were purchased from Novus Biologics (#NBP2-54771, NBP1-77836, AF3797, NBP2-67372). All secondary antibodies used for western blotting in this study were from Jackson Laboratories (#111-035-144, 115-035-062) and fluorescent-

tagged secondary antibodies from Vector Labs (#DI-1094, CY-2500). Human GH was purchased from Pfizer (Genotropin) and recombinant TGF-β1 (#240-B-002) and ELISA kit for TGF-β1 (#DB100B) were procured from R&D systems. SB431542 was purchased from Tocris Bioscience (#1614).

Animal experiments and animal care: Swiss-albino mice were purchased from the National Centre for Laboratory Animal Studies (NCLAS, NIN, Hyderabad). Mice were maintained under 12hr day and night cycles throughout the experimental procedure. After acclimatization animals are grouped into three, control, GH, GH+ SB treatments were performed as detailed. On day fifth of acclimatization, the treatment group received intraperitoneal injections of GH (2mg/kg body weight/day) and the inhibitor group received intraperitoneal injections of SB431542 (1mg/kg body weight/day) 1h prior to the GH treatment. All animals were sacrificed on day 14th post GH treatment, thoroughly perfused with PBS and internal body fixation was done by 4% PFA (paraformaldehyde). Kidneys were collected and one kidney was used for histological analysis and the other kidney was used for isolation of protein and RNA. Institutional Animal Ethics Committee of the University of Hyderabad approved the protocols for animal maintenance and experimentation.

The podocyte GHR knockout (KO) mice (genetic background, C57BL/6J) with targeted deletion of the GHR in podocytes were generated as described before [12]. Diabetes was induced in these mice using streptozotocin and maintained for 8 weeks. We collected urine for analysis before scarifying the animals. The intact kidney was harvested and processed for histological analysis. A portion of the kidney was fixed in 10% phosphate-buffered formalin before paraffin embedding. Another portion was immediately frozen in Tissue-Tek optimum cutting temperature compound before cryo-sectioning. Another kidney was snap frozen in liquid nitrogen and stored at -80° C for protein and RNA extraction. The University of Michigan Animal Care and Use Committee approved all animal protocols pertinent to GHR KO animals.

Cell culture and treatments: Immortalized human podocytes were cultured in 10% serum containing media prepared in RPMI 1640 with 1% antibiotic-antimycotic at 33ºC under 5% CO_2. After cells reached 70% confluence, the cells were transferred to 37ºC and maintained for 6-8 days for differentiation. Differentiated podocytes were used for all treatments. Cells were serum starved in no glucose containing RPMI media for 24hr before being treated by human GH. All treatments were performed in serum-free no glucose media. Before treating cells with GH or TGF-β1, cells were treated with SB431542 for 24h in serum free no glucose medium.

SDS-PAGE & Western Blotting: Unless otherwise mentioned all SDS-PAGE gel percentages were used in this study are 10%. Cell lysates prepared in RIPA lysis buffer and protein estimation was done using Bradford standard method. Equal amounts of protein were loaded and gels were run at 100 volts for 2hrs or until the dye was released. Western blotting was performed using standard methods at 200mA for 1hr at 4ºC and PVDF membrane was used for all western transfers. Blots were incubated with respective primary antibodies for overnight at 4ºC and followed by which the blots were incubated with respective secondary antibodies for 1hr at room temperature. Blots were developed using ECL substrate employing Bio-Rad Versa Doc 5000 MFP and results were analyzed in Image Lab. Further, Band intensities were quantified in Image J software (NIH, Bethesda).

Immunohistochemistry: Paraffin-embedded tissues were cut into 6µm thin sections in Leica systems microtome. Sections were deparaffinized in xylene and rehydrated with ethanol from 100% to 50%. Peroxidase blocking and permeabilization were performed in 30% H_2O_2 for 25min at room temperature on gentle racking. Antigen retrieval was done in Tris-EDTA-Tween buffer at the high micro oven for five minutes thrice at regular intervals of two minutes. Blocking was performed in 5% BSA in PBS for 1hr at room temperature. Sections were incubated with primary antibody for two hours followed by two washes with PBS and incubated with secondary antibody either with fluorescent tagged or HRP (horseradish peroxidase) conjugate. Sections

were developed using DAB stain and counterstained with hematoxylin. All washes are done with PBS. Finally, sections were dehydrated and mounted with DPX mounting media.

Immunofluorescence: Immunofluorescence performed according to the previous protocols available in the literature [12]. Cells were fixed with 4% PFA for 10min on a glass coverslip and permeabilized with 0.5% Triton X-100 for 15min at room temperature. Blocking was performed with 5% BSA in PBS for 1hr and primary antibody was used 1:100 dilution. Followed by secondary antibody labeled with fluorescent tag one at room temperature. Finally, cells were mounted with prolong gold antifade with DAPI purchased from Molecular Probes (#P36941). All washes are done with PBS. Imaging was done in Leica Microsystems trinocular or Zeiss confocal microscopy.

SMAD4-Cignal GFP Reporter Assay: SMAD4 cignal-GFP reporter assay was performed in HEK293T cells according to the earlier published protocols with minor modifications [18]. In a 96 well plate, $6X10^3$cells/well were seeded prior to the day of transfection. Cells were transfected either with SMAD4-GFP, positive control and negative control vectors in triplicates. After transfection cells were left untreated in complete medium for 16h, followed by serum starvation for 12h. Then, cells were treated with TGFβ, GH CM and GH in serum-free medium. After 16h of treatment, images were taken in Olympus 5000 fluorescence microscope and the fluorescence emission spectrum from 510-520nm was recorded in Tecan multiple reader (Infinity 200 Pro) by exciting at 488nm. Fluorescence values were plotted after normalizing with mock test control values.

Transient transfection: All transient transfections were performed according to the manufacturer protocol. 95% confluent HEK293T cells were transfected using lipofectamine 2000, Invitrogen. After 6hr of transection cells were briefly washed with PBS and incubated in 10% serum containing media for 24hr followed by which all treatments were performed in serum free medium.

ELISA for TGF-β1: Cells were serum starved in no glucose containing RMPI 1640 medium for 24h under standard culture conditions. Cells were treated with GH 250 and 500ng concentrations in the starvation medium (not supplement with glucose) for 30min. Briefly, dead cells were removed from the cell supernatants by centrifugation at 16000g for 10min at 4°C and the supernatants were passed through 0.2µm membrane filters. The resultant supernatants were directly subjected to the TGF-β1 activation procedures as the manufacturer's protocol. Activated samples were assayed by indirect sandwich Elisa kit purchased from R&D systems (# DB100B).

Paracellular albumin influx assay: Albumin influx assay was performed in podocytes according to the previous publications. $1.2X10^5$ cells per well were seeded on to the top chamber of the 6-well insert. The wells of the six-well plate were filled with 6ml of RPMI complete medium and incubated under permissive conditions for 24h. Then cells were shifted to 37°C and incubated for five for differentiation into mature podocytes. Followed by which cells were serum starved for 24h and indicated treatments were given to the cells. After 48hr of treatment, cells were washed with PBS supplemented with 1mM MgCl2 and 1mM CaCl2 to preserve cadherin junctions. Then, six-well plates were filled with 6ml of 40mg/ml BSA containing serum-free RPMI medium and the top chamber filled only with 0.7ml of RPMI. After incubation, a small aliquot of a medium from the top chamber was collected to measure BSA influx from bottom to top chamber and concentration was assessed by BCA protein assay method.

Statistics Analysis: Data are presented as standard error mean (SEM). Graphpad Prism 8 software was used to analyze statistical differences between the distributions of two (Unpaired non parametric-Mann Whitney test) or multiple independent samples (Tukey's Multiple comparison test), respectively. $p \leq 0.05$ was considered as significant.

Results:

GH induces the TGF-β/SMAD pathway in human podocytes: Considering both the instrumental role of podocytes in glomerular permselectivity and association of TGF-β1 with glomerular pathophysiology, we investigated the direct action of GH on TGF-β/SMAD pathway in human podocytes. We found that GH (100-500ng/ml) induces TGF-β1 protein levels as analyzed by immunoblotting in human podocytes (Fig 1A&B). Since TGF-β1 is a secretory molecule, we next estimated TGF-β1 content in the conditioned medium obtained from GH treated podocytes in both dose (250 & 500 ng/ml) and time (0-60') dependent manner. We found an increase in TGF-β1 protein levels with GH treatment compared to controls in both the cases, respectively (Fig 1C&D). Further, we also found increased phosphorylation of SMAD 2&3 with GH treatment (0-60') in podocytes (Fig 1E&F). The data suggest that GH elicits TGF-β1 expression and activation of TGF-β1 down-stream signaling in podocytes.

GH induced TGF-β functions in both autocrine and paracrine manner: TGF-β1 is known to act in both autocrine and paracrine manner. To elucidate the paracrine action of GH induced TGF-β1, we treated podocytes with GH and collected conditioned media. Conditioned media from GH-treated podocytes induced phosphorylation of SMAD2 and 3 in podocytes that are naïve to GH (Fig 2A). This suggests the possibility of GH-dependent secretion of TGF-β1 into the conditioned media, which elicited activation of SMAD2/3. TGF-β dependent regulation of its target genes requires interaction of common co-Smad, SMAD4 with activated SMAD2&3 and the localization of SMAD2/3/4 complex to the nucleus. We observed increased accumulation of SMAD4 in the nucleus with either treatment with GH or conditioned media from GH-treated podocytes (Fig2B). We next performed TGF-β neutralization studies in podocytes transfected with GFP expression plasmid under the control of SMAD binding element (SBE). Both, GH and conditioned media from GH treated podocytes induced GFP expression (Fig 2C). However, the

conditioned media from GH treated podocytes that was pre-incubated with anti-TGF-β1 antibody failed to induce GFP expression (Fig 2C&D). Further, to verify the observed effects of GH on activation of SMADs is mediated via GH-dependent secretion of TGF-β1 in podocytes; we employed TGF-βR1 inhibitor, SB431542 (hereafter named as SB). SB is a small molecule that targets the TGF-β signaling pathway by competing for ATP binding domains in the ALK5 (TGF-βR1) receptor [19]. SB treatment significantly reduced the TGF-β1 levels in GH treated podocytes as measured by ELISA (Fig 3A) and immunoblotting (Fig 3B). In addition, we observed reduced phosphorylation of SMAD2&3 (Fig 3C) and decreased nuclear levels of SMAD4 (Fig 3D) in podocytes treated with GH and SB. We next sought to study the functional consequence of GH-dependent expression of TGF-β1 and down-stream activation of SMAD signaling in podocytes. We assessed podocyte permselectivity using a paracellular albumin influx assay. Podocytes treated with GH showed increased permeability to the albumin across podocyte monolayer (Fig 3E). Interestingly, treatment with SB abrogated the observed effect of GH on podocyte permeability (Fig 3E). Together, these data from either direct treatment with GH or from conditioned media from GH-treated podocytes demonstrate that TGF-β1 induced by GH acts in both autocrine and paracrine manner to activate SMAD signaling, which is associated with altered podocyte permeability.

GH elicits podocyte size and regulates expression of ECM components: We next ascertained whether GH induces podocyte cell size. GH treated podocytes show increased cell size compared with podocytes naïve to GH (Fig 4A). Similar to GH, TGF-β1 also induced increase in podocyte cell size (Fig 4A). Changes in the structural organization of the actin cytoskeleton accompany the changes in cell volume. Therefore, we assessed F-actin distribution in podocytes exposed to GH or TGF-β1 and we observed that increased F-actin distribution as assessed with Phalloidin staining (Fig 4B&C). We also found increased

expression of extracellular matrix molecules in podocytes exposed to GH or TGF-β1 compared with cells naïve to these molecules (Fig 4D&E). Together the data suggests that GH and TGF-β1 elicits podocyte cell volume and also increases the production of ECM components. Increased expression of ECM proteins in podocytes is in corroboration with increased thickening of GBM in mice injected with GH (Fig 4D&E Vs. Fig 6A&B).

GH induces renal hypertrophy and proteinuria in mice: To delineate the *in vivo* role of GH on glomerular function we administered GH to mice for two weeks. GH injected mice displayed higher glomerular size (Fig 5A&B). Kidney weight to body weight ratio increased in GH administered mice (Control vs. GH). Histological analysis of kidney from GH injected mice revealed a mild to moderate renal fibrosis, mesangial expansion, synechiae formation between bowman's space and glomerular tufts (Fig 5C). We also noticed a significant decrease in glomerular filtration rate (GFR) in GH injected animals (Fig 5D). Analysis of podocyte architecture by transmission electron microscopy revealed disruption of podocyte foot-processes and thickening of GBM (Fig 6A&B). Urine from GH administered mice has a higher albumin to creatinine ratio (UCAR, Fig 6C) and more abundance of high molecular weight proteins (Fig 6D) compared with control mice. These results demonstrate that excess GH induces glomerular hypertrophy, alterations in podocyte morphology, and impairment of renal function as evidenced by increased UCAR and decreased GFR.

Activation of TGFB/SMAD pathway in GH injected mice: We conducted further analysis to understand the molecular basis for the glomerular hypertrophy and proteinuria in mice administered with GH. We found that TGF-β1 levels were elevated in platelet poor plasma preparations from GH injected mice (Fig 7A). Furthermore, glomerular lysates from GH injected mice showed increased abundance of TGF-β1 protein (Fig 7B&C). Immunohistochemistry analysis revealed that increased expression of TGF-β1 in both glomerulus and renal tubule (Fig

7D). Increased phosphorylation of Smad 2/3 and elevated levels of Smad4 was observed in glomerular lysates from mice administered with GH (Fig 7E and Supplementary Fig 1).

TGF-βR1 inhibitor attenuates GH induced renal anomalies: In order to ascertain that the observed glomerular injury during GH treatment is specifically due to TGF-β1, we employed the SB (SB431542, TGF-βR1 inhibitor) in our further studies. We injected mice with SB prior to the GH treatment as described earlier [20]. We found SB treatment prevented the increase in TGF-β1 levels induced by GH injection in mice (Fig 8A). SB treatment alleviated the GH-induced glomerular hypertrophy, glomerular tuft area, (Fig 8B&C) and concomitant with reduced SMAD2/3 activation (Fig 8D). Furthermore, SB treatment improved proteinuria in the GH-administered animals (Fig 8E). These results suggest that inhibition of TGF-βR1 could at least partially prevent the GH mediated adverse manifestation on glomerular biology and permselectivity.

Lack of GH action on podocytes attenuated SMAD activation: To further elucidate the mechanistic link between GH and TGF-β1/SMAD pathway and observed renal hypertrophy and proteinuria, we generated podocyte-specific GHRKO ($pGHR^{-/-}$) mice. $pGHR^{-/-}$ mice express reduced levels of GHR in podocytes (Fig 9A). There are no noticeable changes in renal manifestations between $pGHR^{-/-}$ mice and $pGHR^{+/-}$ mice. Since elevated GH levels and hyperactive GH/GHR axis is seen in diabetes, particularly type1, we induced diabetes in both $pGHR^{+/-}$ and $pGHR^{-/-}$ mice by injecting streptozotocin as described in methods section. Our results reveal that attenuation of increased kidney size, glomerular hypertrophy, and sclerosis in $pGHR^{-/-}$ mice under diabetic settings (Fig 9B&C). Interestingly, $pGHR^{-/-}$ mice also showed less proteinuria under diabetic conditions (Fig 9D). We found that $pGHR^{+/-}$ mice under diabetic settings showed increased glomerular expression of TGF-β1 levels in the glomerular lysates.

Conversely, diminished expression of TGF-β1 levels were observed in diabetic pGHR$^{-/-}$ mice (Fig 9E). Further, we also observed activated SMAD3 levels in the pGHR+/- mice glomerulus and these levels were further enhanced with STZ-injection. On the other hand, in pGHR$^{-/-}$ animals, pSMAD3 levels were significantly diminished compared to that of diabetic pGHR$^{+/-}$ mice (Fig 9F). These results indicate that lack of podocyte GHR prevented TGF-β1 expression and thus attenuated activation of down-stream signaling such as activation of SMADs.

Discussion:

The major findings of this study are that GH induces TGF-β1 in glomeruli, particularly in podocytes and that podocytes display GH-dependent activation of canonical TGF-β1/SMAD signaling pathway and synthesis of ECM components. GH induces glomerular hypertrophy, sclerosis, and proteinuria in rats whereas inhibition of TGF-β1R prevented GH-induced degenerative changes in glomeruli and improved proteinuria. GH and TGF-β1 impair podocyte permeability as measured paracellular albumin influx assay and this effect was ameliorated by TGF-β1R inhibitor

As described above there are several lines of evidence indicating that abrogation of GH/GHR axis improves renal function and proteinuria in diabetes settings. Excess GH levels and overactivity of GH/GH receptor (GHR) axis is implicated as a causal factor in the renal hypertrophy but the molecular events attributed to this phenotype remains elusive. It is not clear whether GH's actions on renal physiology and function are due to the direct action of GH on the kidney or indirect actions mediated via hemodynamic changes. Earlier, our group demonstrated the presence of GHR on the podocytes enabling direct actions of GH on glomerular function [12]. We also reported that podocytes treated with GH induce Smad interacting protein 1 (SIP1), also known as zinc finger E-box binding homeobox [11] and TGFBIp [10]. We continued our quest of understanding the crucial role of GH on glomerular biology. In the current study, we

investigated the mechanism of GH induced renal hypertrophy and proteinuria by activation of TGF-β1/SMAD signaling. The two major possibilities for tissue hypertrophy could be hyperplasia of individual cells or accumulation of extracellular matrix. We did not observe podocyte proliferation by GH and ruled out the possibility of podocyte hyperplasia. The other possibility is the accumulation of ECM components. GH-dependent increase in TGF-β1 and resultant accumulation of ECM molecules may contribute to the glomerular hypertrophy in GH administered mice. Our data suggest that GH-dependent secretion of TGF-β1 elicits its action in both autocrine and paracrine manner. Direct treatment with GH induced GFP expression (cloned under putative SMAD binding element) and CM-GH also elicited GFP expression. Former one suggests autocrine and later suggest paracrine action of TGF-β1 in podocytes. Neutralization of TGF-β1 with antibodies abolished the SMAD4 activation potential of CM-GH treated podocytes (Fig 2C). SMAD pathway activation and SMAD4 nuclear localization in response to GH further support our hypothesis that GH induces TGF-β/SMAD signaling.

TGF-β, a hypertrophic and prosclerotic cytokine plays a pivotal role in morphologic manifestations and clinical characteristic of DN. It was shown that TGF-β induces podocyte apoptosis by activation of smad7 that in turn inhibits signaling by NF-κB [21]. GH exerts mild glomerulosclerosis and interstitial fibrosis in diabetic Sprague-Dawley male rats and this renal injury is associated with a marginal elevation in TGF-β1 levels [5]. Renal hypertrophy was reported in patients with excess GH and in GH transgenic animals whereas neutralization of TGF-β using anti-TGF-β1 antibody prevents renal hypertrophy, which is concurrent with inhibition of ECM molecules expression [22]. Acute synthesis and deposition of ECM molecules in the GBM region associated with glomerular hypertrophy [23, 24]. In the present study, we also observed increased expression of ECM molecules in GH treated mice. Furthermore, our study reiterates earlier observations that GH induces glomerular hypertrophy and proteinuria as demonstrated by increased UCAR, decreased GFR and extensive proteinuria. We have demonstrated here that perturbing the TGF-βR1/SMAD pathway by TGF-βR1 inhibitor (SB)

prevented renal hypertrophy and proteinuria. It is noteworthy that SB attenuated TGF-β1 levels in response to GH in the mice demonstrating the autoregulation of TGF-β1. It should be noted that administration of neutralizing TGF-β antibodies decreased the total production of TGF-β [22]. It is also interesting to note that suppressing JAK2, an immediate downstream target of GH, reduced the TGF-β transcript levels in mice [25].

GH transgenic mice displayed significant effacement in podocyte foot processes that resulted in impaired glomerular function [6]. In this study, we observed altered podocyte permeability to BSA as evidenced by paracellular influx assay performed with podocyte monolayers treated either with GH CM or TGF-β conditions. Moreover, podocytes exposed to GH CM that are already treated with SB inhibitor reduces phosphorylation of SMAD2&3. SMAD4 nuclear shuttling also was prevented by treatment with SB inhibitor in these conditions. These observations are correlated with the diminished levels of TGF-β1 in the podocytes exposed to GH in the presence of SB inhibitor. These results further support our hypothesis that TGF-β is regulating its own protein synthesis in an autoregulatory loop which involves SMADs activation. However, to support this hypothesis additional studies are required.

GH/GHR axis has been a potential target to prevent kidney injury in experimental diabetic animal models [26]. STZ-induced diabetic rats administered either with octreotide and lanreotide, a somatostatin analog protected mice from developing renal hypertrophy and proteinuria [26]. Diabetic mice administered with pegvisomant, a functional GHR antagonist protected mice from the development of DN [26]. Similarly, whole body GHR/ binding protein (BP) gene disruption protected mice against the development of DN [7]. Mice overexpressing JAK2, an immediate target of GH/GHR axis in podocytes resulted in thickening of GBM and foot process effacement [27]. Therefore, we hypothesized that targeted deletion of GHR in podocytes may prevents renal hypertrophy and proteinuria in experimental diabetic mice. We observed that pGHR-/- mice protected from the development of DN whereas pGHR$^{+/-}$ mice

developed significant renal hypertrophy, glomerulosclerosis, and proteinuria in the settings of STZ-induced diabetes. Increased levels of TGF-β1 were observed in the glomerular sections from pGHR+/- mice under diabetic settings. Contrastingly, pGHR-/- mice do not display TGF-β staining in immunohistochemistry analysis. These studies demonstrated the clear role of TGF-β1/SMAD pathway in mediating the GH induced diabetic renal changes.

TGF-β/SMAD pathway activation is crucial in most of the kidney diseases but the molecular cues for its expression and activation are remains unclear. Previous studies propose that high glucose and angiotensin II induces TGF-β1 expression in mesangial cells, but in the podocytes, angiotensin II do not have any effect on TGF-β expression. Moreover, it is largely uncertain whether podocytes secrete TGF-β in response to damage such as chronic glomerular disease [28]. Our study provides evidence that glomerular podocyte is a source of TGF-β1 and they secrete TGF-β1 upon stimulus by GH, which manifest in glomerular injury and eventual proteinuria. Based on the current study and earlier studies, we conclude that GH induces TGF-β1 expression and it could be implicated as a causative factor in the development of renal hypertrophy. Several clinical trials investigating the effectiveness of inhibiting TGF-β1 in the treatment of focal glomerulosclerosis, myelofibrosis, and pulmonary fibrosis (Clinicaltrials.gov).

Acknowledgments: We acknowledge the Science and Engineering Research Board (EMR/2015/002076) for providing funding to AKP. DM and RN are recipients of a research fellowship from the University Grants Commission. Authors thank Dr. Arun Kumar Kota for providing SMAD4-GFP signal reporter assay kit.

Author Contributions: DM, RN, and AKP performed experiments. DM and AKP analyzed the data. RKM generated pGHR KO mice. DM, RKM, and AKP wrote the manuscript.

Figure legends

GH treatment induces TGF-β/SMAD pathway in podocytes. Human podocytes were treated with GH in dose-dependent manner and cell lysates subjected to 8% SDS-PAGE and western blotting performed to assess TGF-β1 expression (A) and quantification of TGF-β1 expression by Image J. Actin was used as loading control and the TGF-β expression was normalized to β-actin (B). TGF-β1 levels were estimated by ELISA in conditioned media from podocytes treated with GH in dose and time dependent manner (C&D). Western blotting analysis for TGF-β1 and SMAD2/3 expression in podocytes exposed to GH (500ng/ml) for varying periods of time (E). Actin was used as loading control and band intensity of TGF-β was normalized to actin and pSMAD2 and 3 were normalized to total SMAD2/3 (F). Statistical differences analyzed via one-way Anova. Each experiment was performed three times and the p value <0.05 considered as significant, represented by * ($p<0.05$), ** ($p<0.003$).

Figure 2: Autocrine/paracrine activity of GH induced TGF-β1 in podocytes. Conditioned media (CM-GH) from podocytes treated with GH for 30 min was collected, briefly centrifuged to remove debris and added to the podocytes that are naïve to the GH treatment. Total cell extracts prepared from podocytes treated with CM-GH and assessed for activation of SMADs (A). Experiment was repeated at least three times. SMAD-GFP signal reporter assay was performed in HEK 293T cells treated for 12h either with GH, GH CM, and rTGF-β1. GH CM was prepared by treating podocytes with GH for 30min and the cell supernatants were directly used in treatment of HEK 293T cells (B). GFP fluorescence intensities were measured in Teckan mutiplate reader and plotted after normalizing with the mock test control (C). Experiment was performed two times and each bar represents the mean fluorescence of each experiment. $p<0.006$ is applicable to all data set points. Statistical differences analyzed by one-sample t-test and $p<0.006$ indicates **. SMAD4 nuclear localization in podocytes treated with or without GH and CM-GH for 30min (D).

Figure 3: SB treatment attenuated SMAD4 nuclear localization in GH treated podocytes. Cells treated with GH for 30min in the presence or absence of SB431542 and cell culture supernatants were collected from all experimental setups and processed as indicated above and subjected to ELISA for measuring the levels of TGF-β1 protein (A). Cell debris free-culture supernatants were concentrated using 20% trichloroacetic acid precipitation method and 20µg

of concentrate was loaded on to the SDS-PAGE. Followed by western transfer, the blot was probed with the TGF-β1 antibody. Ponceau stained blot was provided to express the equal amount of protein was loaded (B). Western blotting analysis of control or GH treated podocytes in the presence or absence of SB treatment for the activation of SMAD2 and 3 (C). Each experiment was performed at least twice and *** indicates $p<0.001$. SMAD4 localization studies performed in podocytes with or without GH treatment in the presence of SB inhibitor (D). Paracellular albumin influx assay performed in podocytes treated with either GH or rTGF-β1 in the presence or absence of SB inhibitor (E). BSA protein levels are estimated by BCA protein assay kit at varying time points. Experiment was performed twice and statistical differences were analyzed by two-way Anova (Tukey's mutliple comparision test). * indicates $p<0.05$.

Figure 4: GH regulates ECM expression partly by TGF-β induction. Phase contrast microscopic images of podocytes treated with GH or TGF-β (A). Phalloidin staining of podocytes treated with GH or TGF-β (B) and quantification of volume of cell using image J (C). Cells were primarily fixed on coverslip with 4% paraformaldehyde and phalloidin staining was performed using Tritc labeled phalloidin to estimate the size of the podocytes. (A). Images were acquired in Trinocular microscope at 40X magnification. Ten cells from each image and ten images per group analyzed by image J to derive the mean cell area in arbitrary units (a.u). Western blotting analysis for the ECM molecules treated with GH (D) and their band intensities quantification by Image J (E).

Figure5: GH induces glomerular hypertrophy and impairs renal function: GH induces glomerular hypertrophy and impairs renal function: Bright field images of isolated glomeruli from GH injected animals (A). Bright filed images of 20 glomeruli from each group, control and GH injected mice are analyzed using Image J software, NIH (B). Representative image for renal cortical sections stained with PAS showing enlarged glomeruli with hypercellularity and mild fibrosis in GH treated group (C). Urinary albumin to creatinine ratio measured in control and GH injected animals (D). Urine samples analyzed in SDS-PAGE gels using silver staining method (E). GFR estimated in GH injected animals using Fit-GFR Inulin kit developed by BioPAL (F). n= 5-6 per group; statistical differences analyzed via non-parametric t-test and * inicates $p<0.05$.

Figure 6: Histological analysis: Paraformaldehyde perfused tissues were primarily fixed in 2.5% glutaraldehyde for overnight and the tissues were processed for TEM sectioning as indicated in methods section. TEM sections were prepared from GH and other subjects, and imaging were done in Tecnai G2 S Twin (200kV) system (A). Four images from each group was used to quantify GBM thickness in Image J and the values represent the area as the thickness

of the GBM in arbitrary units (a.u) (B). Each dot represents the mean area of one mice and * indicates p<0.02 and ** indicate p<0.008. Statistical difference was derived from one-way Anova using Tukey's multiple comparison test.

Figure 7: GH treatment induces the TGF-β/SMAD pathway *in vivo*: Platelet poor plasma preparations from GH injected and control animals were subjected to ELISA to measure TGF-β1 levels (A). Western blotting analysis of TGF-β1 in the glomerular lysates from GH injected and control animals (B). Quantification of band intensity with Image J analysis shown in (C). Immunohistochemical analysis of TGF-β1 in paraffin-embedded sections obtained from GH and control animals and developed with DAB. (E) Western blotting analysis demonstrating SMADs activation in the glomerular lysates from control and GH injected animals by using the phospho-specific antibodies (E). Statistical differences analyzed via non-parametric t-test, *, and **, indicates p<0.05, 0.01, respectively.

Figure8: SB431542 administration prevented renal injury: Plasma preparations of GH injected and other experimental group animals were subjected to ELISA for measuring TGF-β1 levels (A). Kidney cortical sections prepared from GH injected and other animal groups and subjected to PAS staining (B). Ten glomeruli from each animal were taken from all the experimental groups to derive the glomerular area in the Image J software and expressed as mean glomerular area (a.u) (C). Each dot represents mean glomerular area from one mouse and *** indicates p<0.0001. Western blotting analysis for activated SMADs in the glomerular preparations from mice treated with GH and other groups (D). Urine samples collected from control and experimental groups subjected to direct urine analysis using silver staining method. 10µg of protein was loaded onto the SDS-PAGE (E).

Figure 9: Targeted deletion of GHR in podocytes prevented GH induced renal abnormalities. Total RNA isolated from liver and kidney tissues were subjected for cDNA synthesis and total GHR transcripts were measured by qPCR (A). Similarly, GHR expression was determined by qPCR in total RNA from isolated glomerular podocytes of pGHR+/- and pGHR-/- animals. Each bar represents the relative expression of GHR from three mice. Kidney images and representative H&E staining of the glomerular sections from pGHR+/- and pGHR-/- under diabetic settings (B). 10 glomerulus from each group analyzed and the mean values were plotted as relative glomerular area in arbitrary units (a.u) (C). Each dot indicates one animal and *** represents p<0.0001. Write about Synaptopodin and GHR expression (D). Urine sample as from pGHR+/- and pGHR-/- mice were loaded on to 10% SDS-PAGE and performed silver staining (E). Total RNA extracts form pGHR+/- and pGHR-/- injected with STZ were used make

cDNA and TGF-β1 transcript levels were analyzed by qPCR (F). Each dot represents one animal and **** indicates p<0.0001. Glomerular sections were probed with WT1 and pSMAD3 antibodies and performed co-immunofluorescence study using differential fluorescent-tagged secondary antibodies (G). Images were acquired in Trinocular Leica Microscopic systems at 40X magnification.

References:

1. Anil Kumar, P., et al., *Molecular and cellular events mediating glomerular podocyte dysfunction and depletion in diabetes mellitus.* Front Endocrinol (Lausanne), 2014. **5**: p. 151.
2. Mukhi, D., et al., *Novel Actions of Growth Hormone in Podocytes: Implications for Diabetic Nephropathy.* Front Med (Lausanne), 2017. **4**: p. 102.
3. Kumar, P.A., F.C. Brosius, 3rd, and R.K. Menon, *The glomerular podocyte as a target of growth hormone action: implications for the pathogenesis of diabetic nephropathy.* Curr Diabetes Rev, 2011. **7**(1): p. 50-5.
4. Pasupulati, A.K. and R.K. Menon, *Growth hormone and chronic kidney disease.* Curr Opin Nephrol Hypertens, 2019. **28**(1): p. 10-15.
5. Whitney, J.L., et al., *Growth hormone exacerbates diabetic renal damage in male but not female rats.* Biol Sex Differ, 2013. **4**: p. 12.
6. Blutke, A., et al., *Growth hormone (GH)-transgenic insulin-like growth factor 1 (IGF1)-deficient mice allow dissociation of excess GH and IGF1 effects on glomerular and tubular growth.* Physiol Rep, 2016. **4**(5).
7. Bellush, L.L., et al., *Protection against diabetes-induced nephropathy in growth hormone receptor/binding protein gene-disrupted mice.* Endocrinology, 2000. **141**(1): p. 163-8.
8. Flyvbjerg, A., et al., *Octreotide administration in diabetic rats: effects on renal hypertrophy and urinary albumin excretion.* Kidney Int, 1992. **41**(4): p. 805-12.
9. Auriemma, R.S., et al., *The kidney in acromegaly: renal structure and function in patients with acromegaly during active disease and 1 year after disease remission.* Eur J Endocrinol, 2010. **162**(6): p. 1035-42.
10. Chitra, P.S., et al., *Growth Hormone Induces Transforming Growth Factor-Beta-Induced Protein in Podocytes: Implications for Podocyte Depletion and Proteinuria.* J Cell Biochem, 2015. **116**(9): p. 1947-56.
11. Kumar, P.A., et al., *Growth hormone (GH)-dependent expression of a natural antisense transcript induces zinc finger E-box-binding homeobox 2 (ZEB2) in the glomerular podocyte: a novel action of gh with implications for the pathogenesis of diabetic nephropathy.* J Biol Chem, 2010. **285**(41): p. 31148-56.
12. Reddy, G.R., et al., *Identification of the glomerular podocyte as a target for growth hormone action.* Endocrinology, 2007. **148**(5): p. 2045-55.
13. Chang, A.S., et al., *Transforming growth factor-beta1 and diabetic nephropathy.* Am J Physiol Renal Physiol, 2016. **310**(8): p. F689-F696.
14. Langham, R.G., et al., *Transforming growth factor-beta in human diabetic nephropathy: effects of ACE inhibition.* Diabetes Care, 2006. **29**(12): p. 2670-5.

15. Qiao, Y.C., et al., *Changes of transforming growth factor beta 1 in patients with type 2 diabetes and diabetic nephropathy: A PRISMA-compliant systematic review and meta-analysis.* Medicine (Baltimore), 2017. **96**(15): p. e6583.
16. Hathaway, C.K., et al., *Low TGFbeta1 expression prevents and high expression exacerbates diabetic nephropathy in mice.* Proc Natl Acad Sci U S A, 2015. **112**(18): p. 5815-20.
17. Voelker, J., et al., *Anti-TGF-beta1 Antibody Therapy in Patients with Diabetic Nephropathy.* J Am Soc Nephrol, 2017. **28**(3): p. 953-962.
18. Maruthi, M., et al., *Modulation of host cell SUMOylation facilitates efficient development of Plasmodium berghei and Toxoplasma gondii*. Cell Microbiol, 2017. **19**(7).
19. Callahan, J.F., et al., *Identification of novel inhibitors of the transforming growth factor beta1 (TGF-beta1) type 1 receptor (ALK5).* J Med Chem, 2002. **45**(5): p. 999-1001.
20. Grygielko, E.T., et al., *Inhibition of gene markers of fibrosis with a novel inhibitor of transforming growth factor-beta type I receptor kinase in puromycin-induced nephritis.* J Pharmacol Exp Ther, 2005. **313**(3): p. 943-51.
21. Schiffer, M., et al., *Apoptosis in podocytes induced by TGF-beta and Smad7.* J Clin Invest, 2001. **108**(6): p. 807-16.
22. Sharma, K., et al., *Neutralization of TGF-beta by anti-TGF-beta antibody attenuates kidney hypertrophy and the enhanced extracellular matrix gene expression in STZ-induced diabetic mice.* Diabetes, 1996. **45**(4): p. 522-30.
23. Osterby, R. and H.J. Gundersen, *Fast accumulation of basement membrane material and the rate of morphological changes in acute experimental diabetic glomerular hypertrophy*. Diabetologia, 1980. **18**(6): p. 493-500.
24. Osterby, R., et al., *Growth hormone enhances basement membrane thickening in experimental diabetes. A preliminary report*. Diabetologia, 1978. **15**(6): p. 487-9.
25. Wang, X., et al., *Inhibition of the Jak/STAT signaling pathway prevents the high glucose-induced increase in tgf-beta and fibronectin synthesis in mesangial cells.* Diabetes, 2002. **51**(12): p. 3505-9.
26. Flyvbjerg, A., et al., *Inhibitory effect of a growth hormone receptor antagonist (G120K-PEG) on renal enlargement, glomerular hypertrophy, and urinary albumin excretion in experimental diabetes in mice.* Diabetes, 1999. **48**(2): p. 377-82.
27. Zhang, H., et al., *Podocyte-specific JAK2 overexpression worsens diabetic kidney disease in mice.* Kidney Int, 2017. **92**(4): p. 909-921.
28. Lee, H.S. and C.Y. Song, *Differential role of mesangial cells and podocytes in TGF-beta-induced mesangial matrix synthesis in chronic glomerular disease.* Histol Histopathol, 2009. **24**(7): p. 901-8.

Fig 1

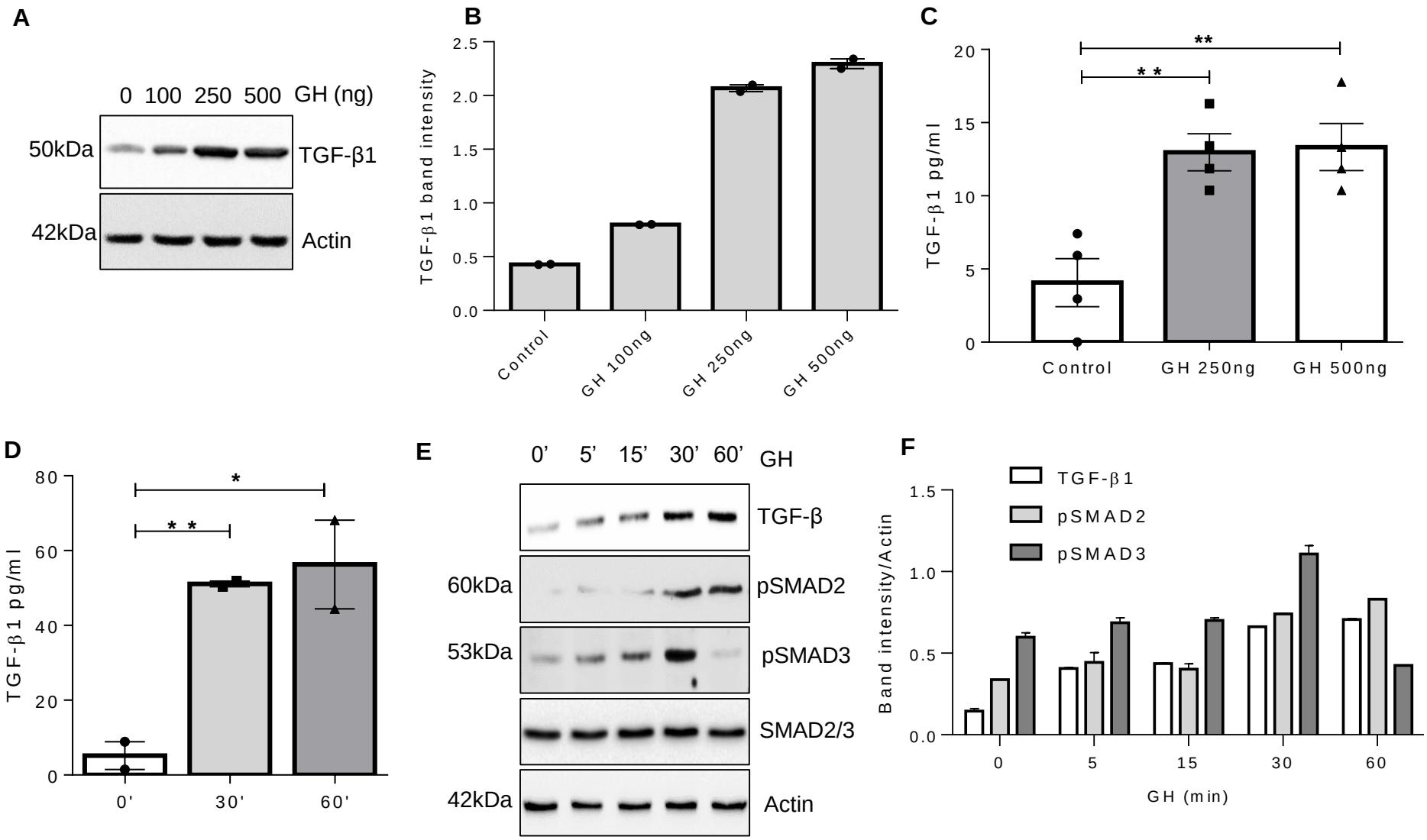
A
0 100 250 500 GH (ng)
50kDa
TGF-β1
42kDa
Actin
B
TGF-β1 band intensity
2.5
2.0
1.5
1.0
0.5
0.0
Control
GH 100ng
GH 250ng
GH 500ng
C
TGF-β1 pg/ml
20
15
10
5
0
**
**
Control
GH 250ng
GH 500ng
D
TGF-β1 pg/ml
80
60
40
20
0
*
**
0'
30'
60'
E
0' 5' 15' 30' 60' GH
TGF-β
60kDa
pSMAD2
53kDa
pSMAD3
SMAD2/3
42kDa
Actin
F
TGF-β1
pSMAD2
pSMAD3
Band intensity/Actin
1.5
1.0
0.5
0.0
0
5
15
30
60
GH (min)

Fig 2

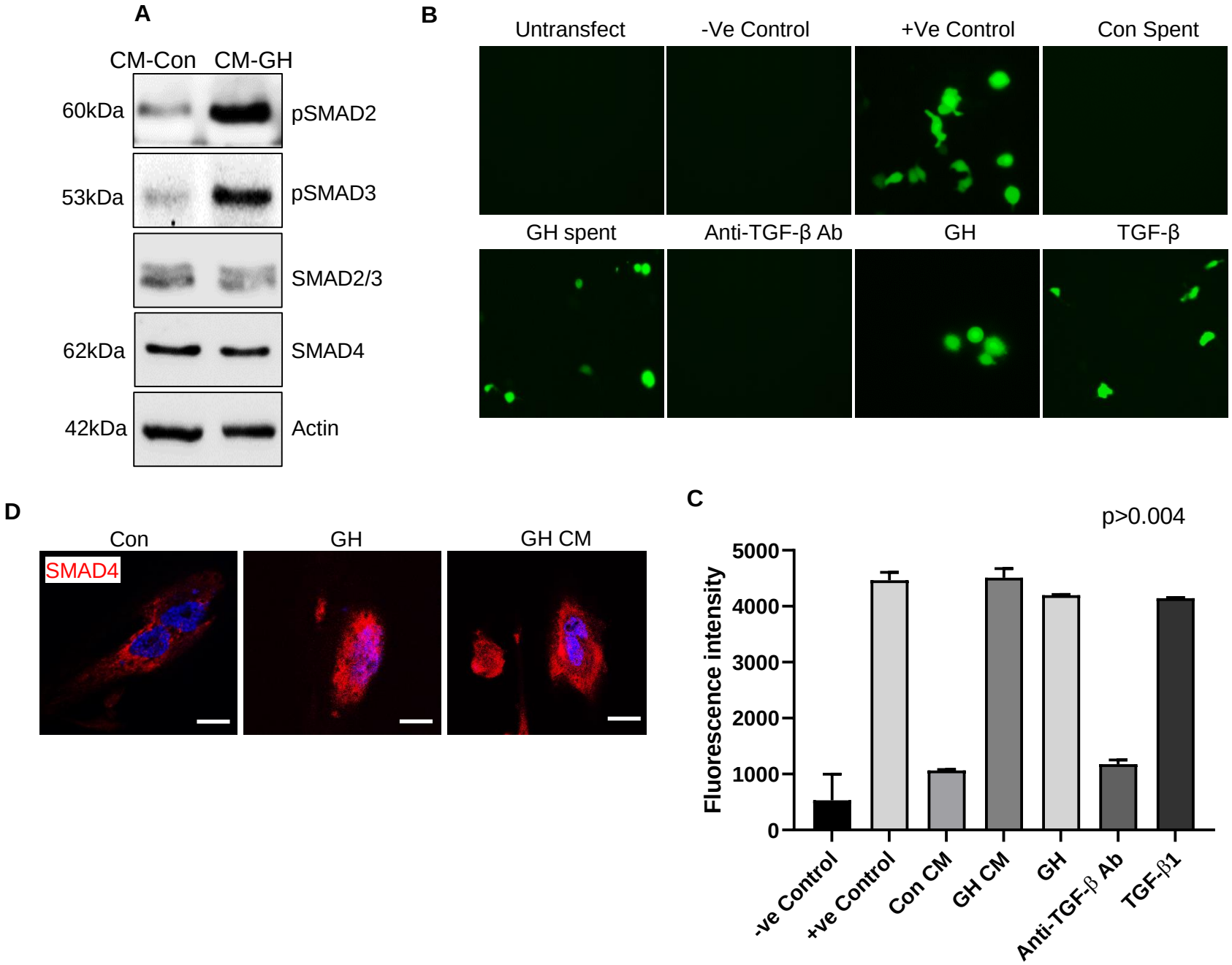
A
CM-Con
CM-GH
60kDa
pSMAD2
53kDa
pSMAD3
SMAD2/3
62kDa
SMAD4
42kDa
Actin
B
Untransfect
-Ve Control
+Ve Control
Con Spent
GH spent
Anti-TGF-β Ab
GH
TGF-β
D
Con
GH
GH CM
SMAD4
C
p>0.004
Fluorescence intensity
5000
4000
3000
2000
1000
0
-ve Control
+ve Control
Con CM
GH CM
GH
Anti-TGF-β Ab
TGF-β1

Fig 3

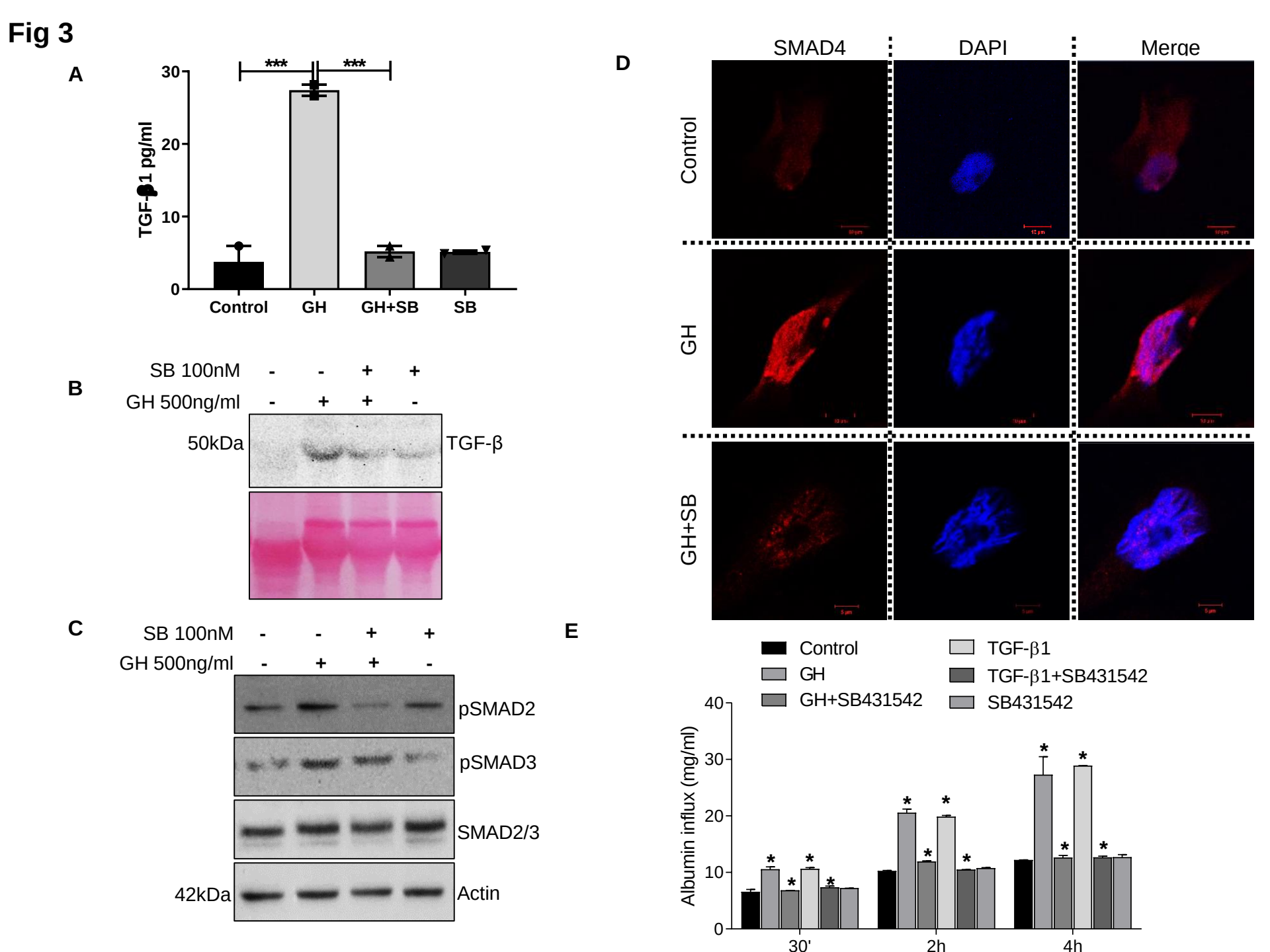
A
TGF-β1 pg/ml
30
20
10
0
***
***
Control
GH
GH+SB
SB
B
SB 100nM - - + +
GH 500ng/ml - + + -
50kDa
TGF-β
C
SB 100nM - - + +
GH 500ng/ml - + + -
pSMAD2
pSMAD3
SMAD2/3
42kDa
Actin
D
SMAD4
DAPI
Merge
Control
GH
GH+SB
E
Control
GH
GH+SB431542
TGF-β1
TGF-β1+SB431542
SB431542
Albumin influx (mg/ml)
40
30
20
10
0
30'
2h
4h

Fig 4

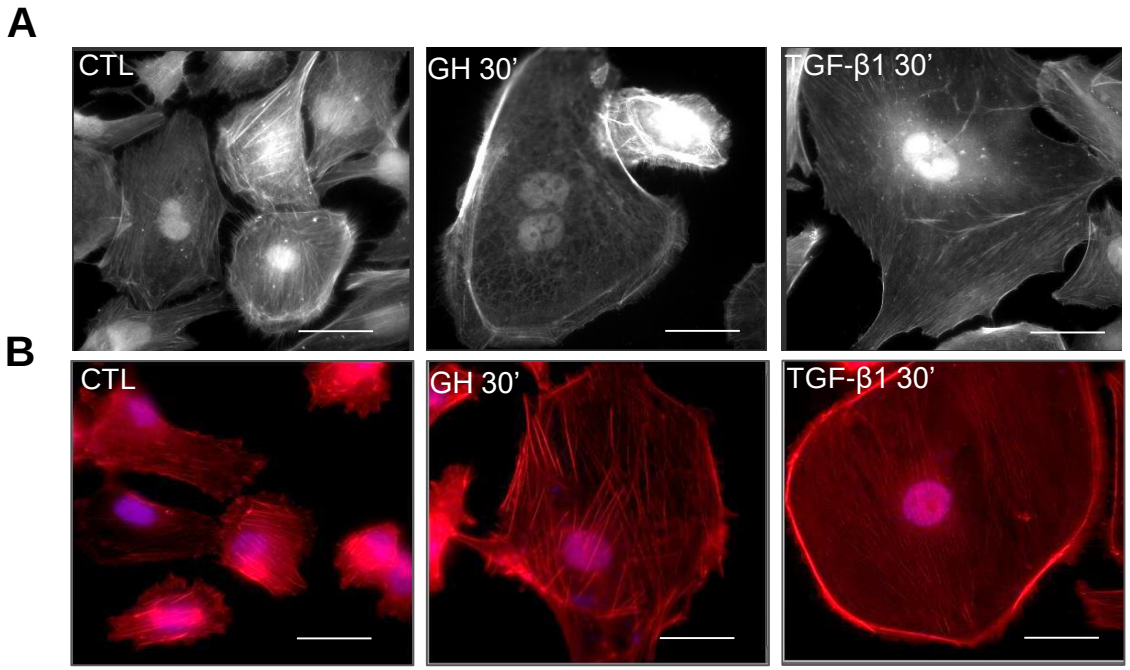
A
CTL
GH 30'
TGF-β1 30'
B
CTL
GH 30'
TGF-β1 30'

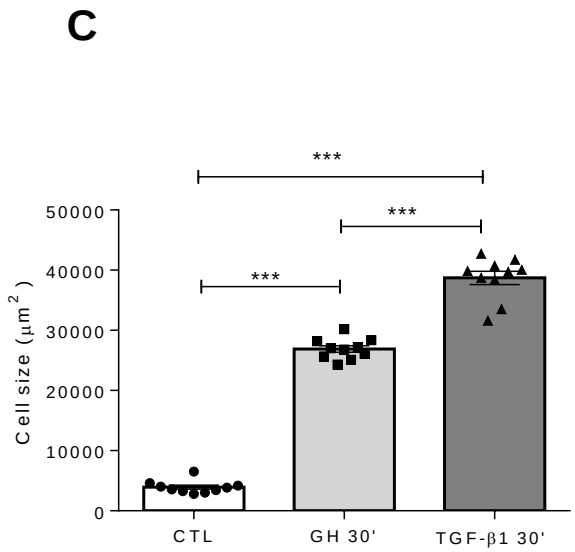
C
***
***
***
50000
40000
30000
20000
10000
0
Cell size (μm²)
CTL
GH 30'
TGF-β1 30'

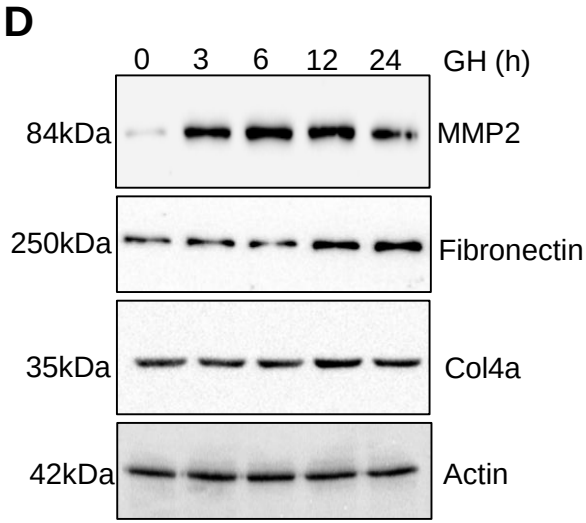
D
0
3
6
12
24
GH (h)
84kDa
MMP2
250kDa
Fibronectin
35kDa
Col4a
42kDa
Actin

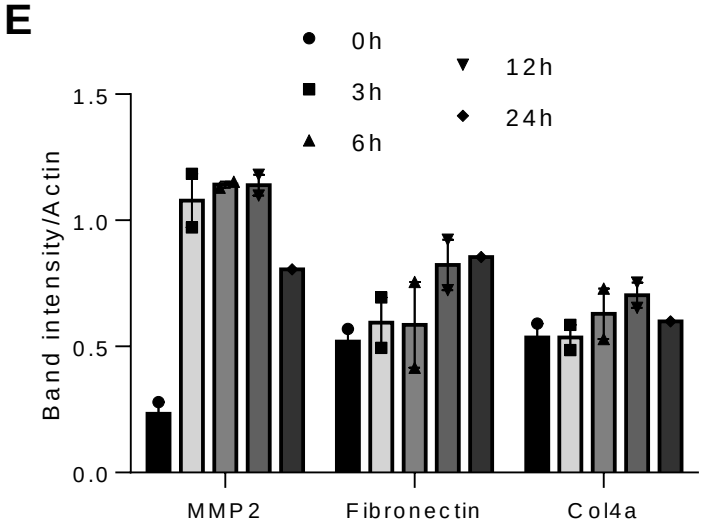
E
0h
3h
6h
12h
24h
1.5
1.0
0.5
0.0
Band intensity/Actin
MMP2
Fibronectin
Col4a

Fig 5

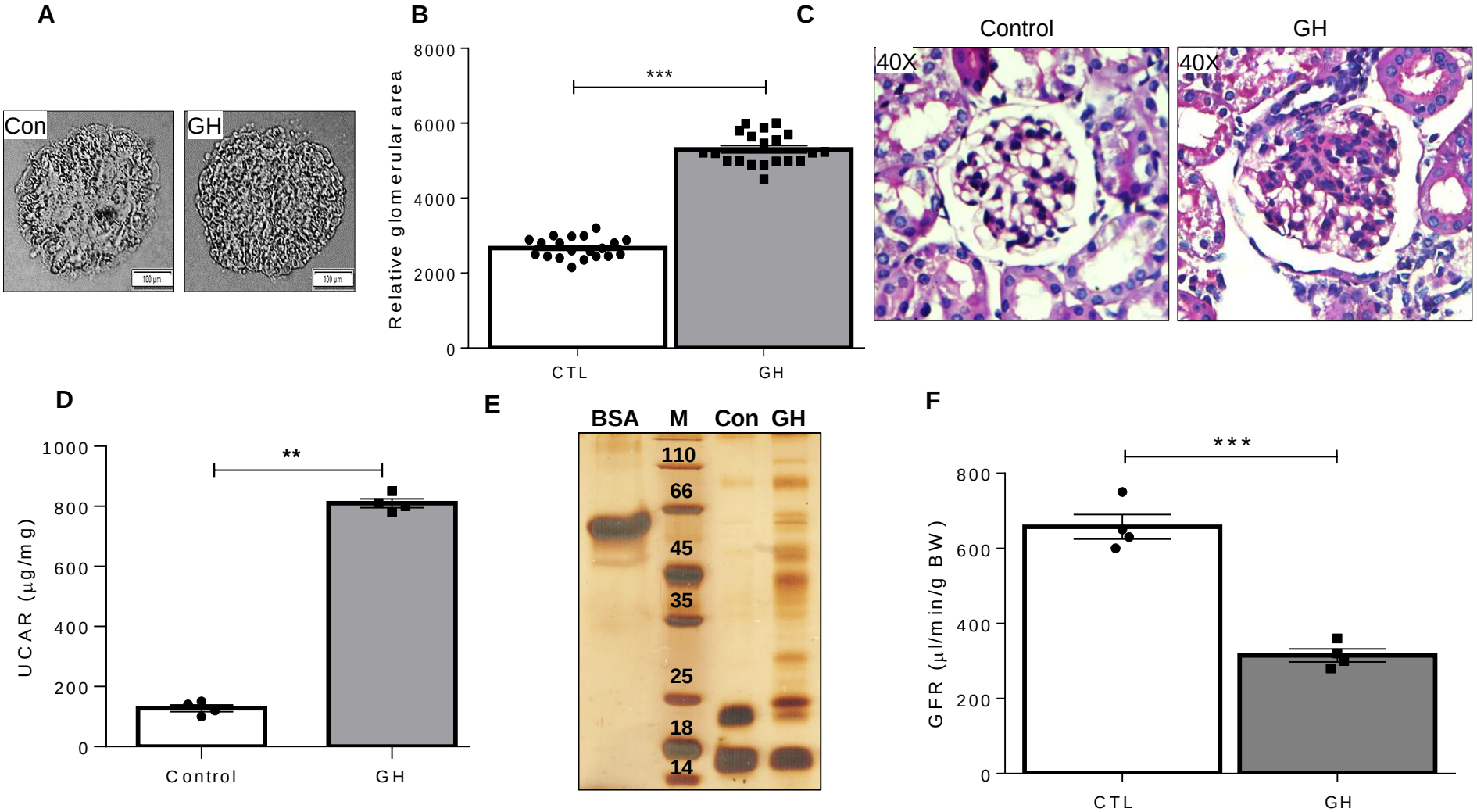
A
Con
GH
100 µm
B
Relative glomerular area
8000
6000
4000
2000
0
***
CTL
GH
C
Control
GH
40X
40X
D
UCAR (µg/mg)
1000
800
600
400
200
0
**
Control
GH
E
BSA
M
Con
GH
110
66
45
35
25
18
14
F
GFR (µl/min/g BW)
800
600
400
200
0
***
CTL
GH

Fig 6:

A

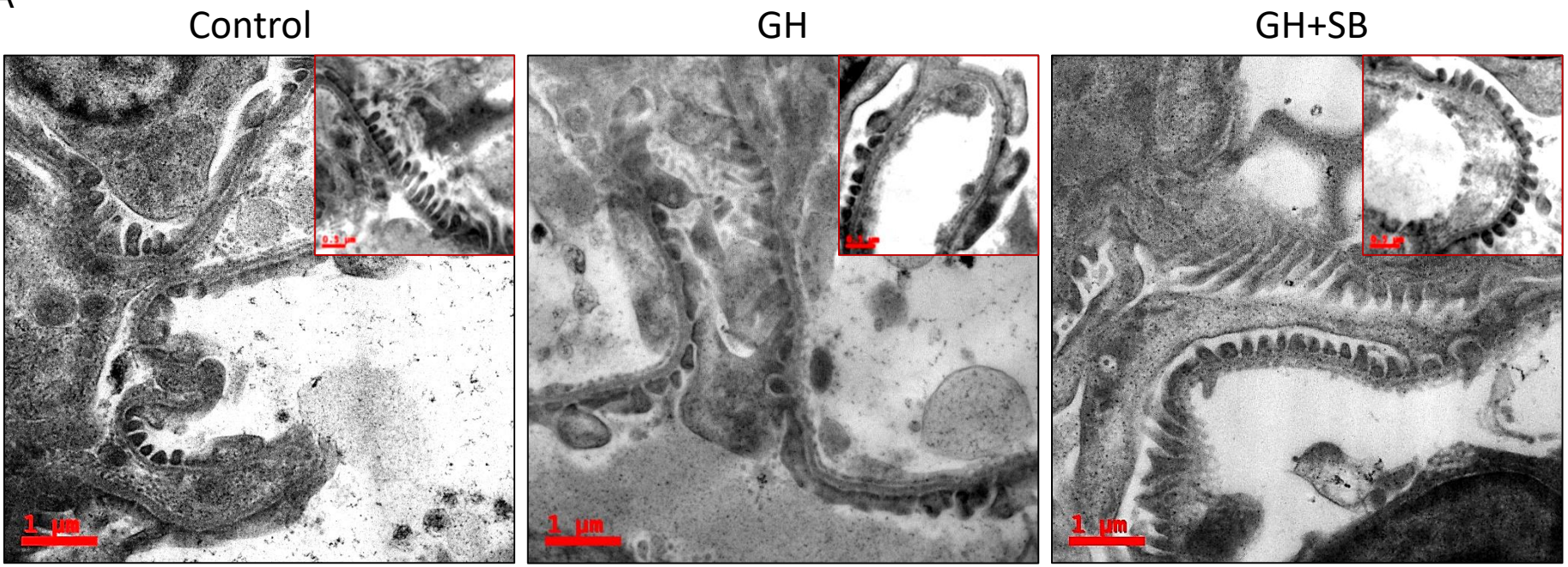
Control
GH
GH+SB
1 µm
1 µm
1 µm

B

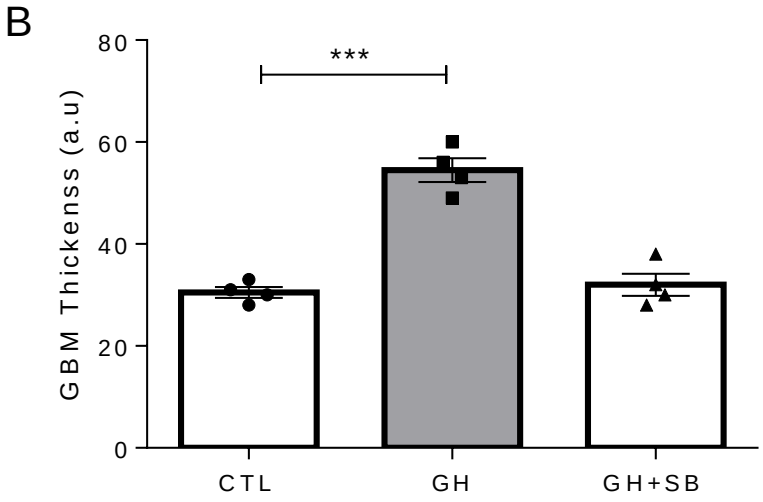
***
GBM Thickenss (a.u)
80
60
40
20
0
CTL
GH
GH+SB

Fig 7

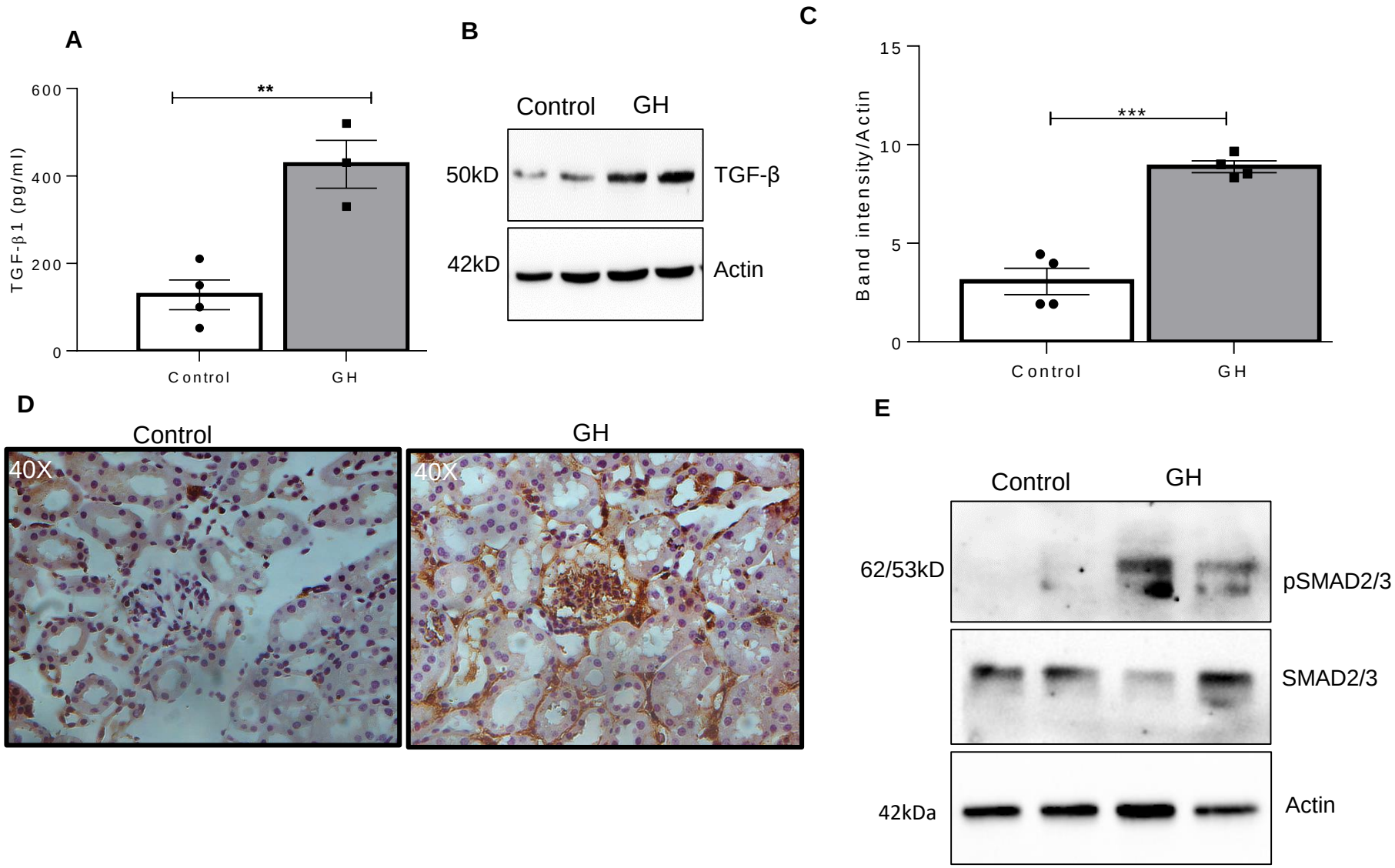
A
600
400
200
0
TGF-β1 (pg/ml)
**
Control
GH
B
Control
GH
50kD
TGF-β
42kD
Actin
C
15
10
5
0
Band intensity/Actin
***
Control
GH
D
Control
GH
40X
40X
E
Control
GH
62/53kD
pSMAD2/3
SMAD2/3
42kDa
Actin

Fig 8

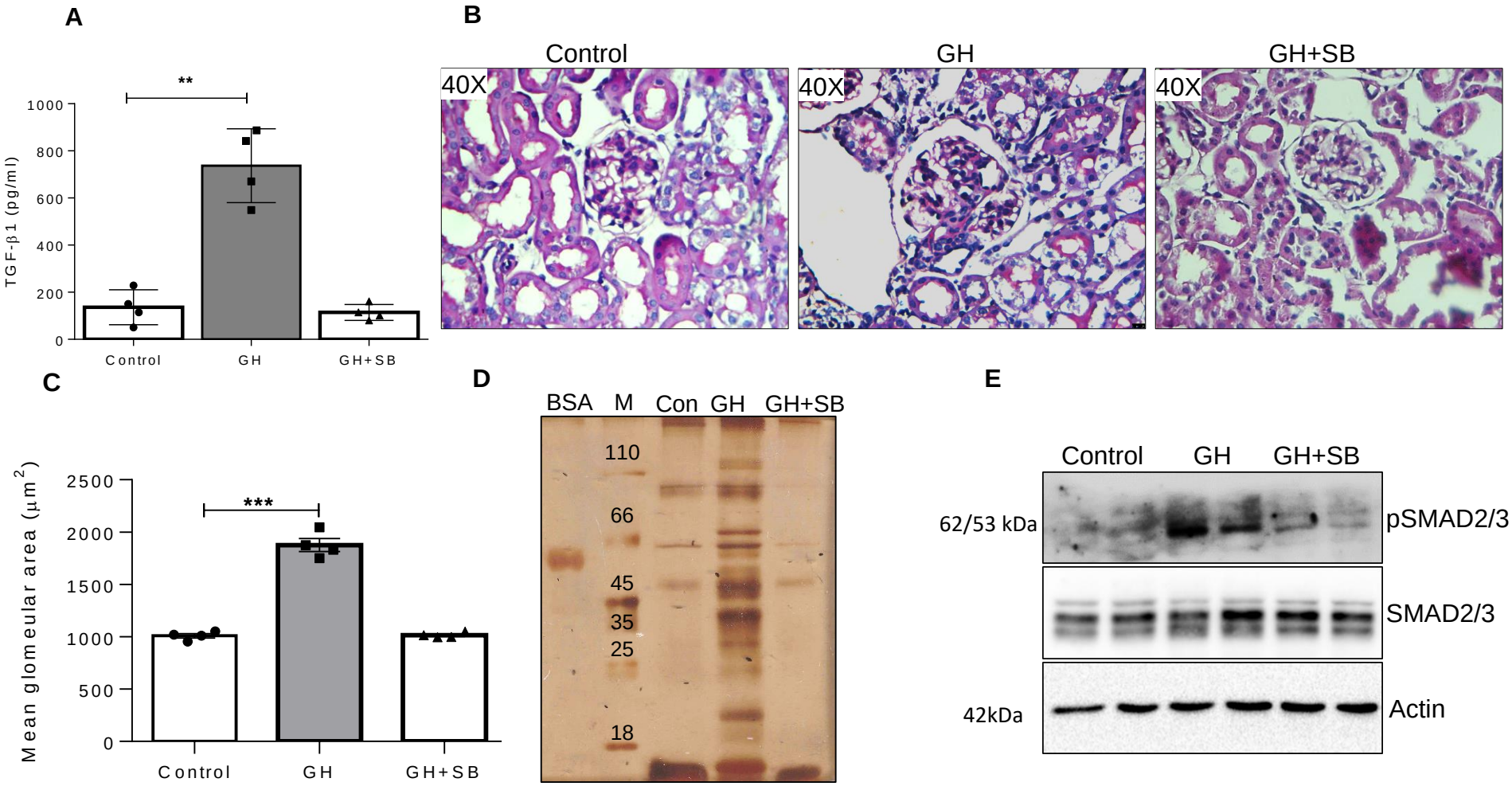
A
**
1000
800
600
400
200
0
TGF-β1 (pg/ml)
Control
GH
GH+SB
B
Control
GH
GH+SB
40X
40X
40X
C
***
2500
2000
1500
1000
500
0
Mean glomeular area (μm2)
Control
GH
GH+SB
D
BSA
M
Con
GH
GH+SB
110
66
45
35
25
18
E
Control
GH
GH+SB
62/53 kDa
pSMAD2/3
SMAD2/3
42kDa
Actin

Fig 9

A

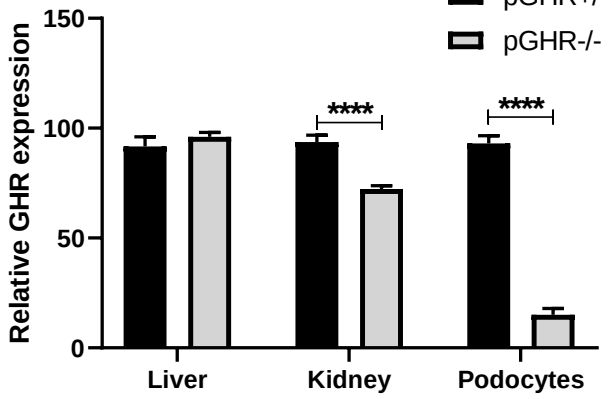
pGHR+/-
pGHR-/-
Relative GHR expression
150
100
50
0
****
****
Liver
Kidney
Podocytes

D

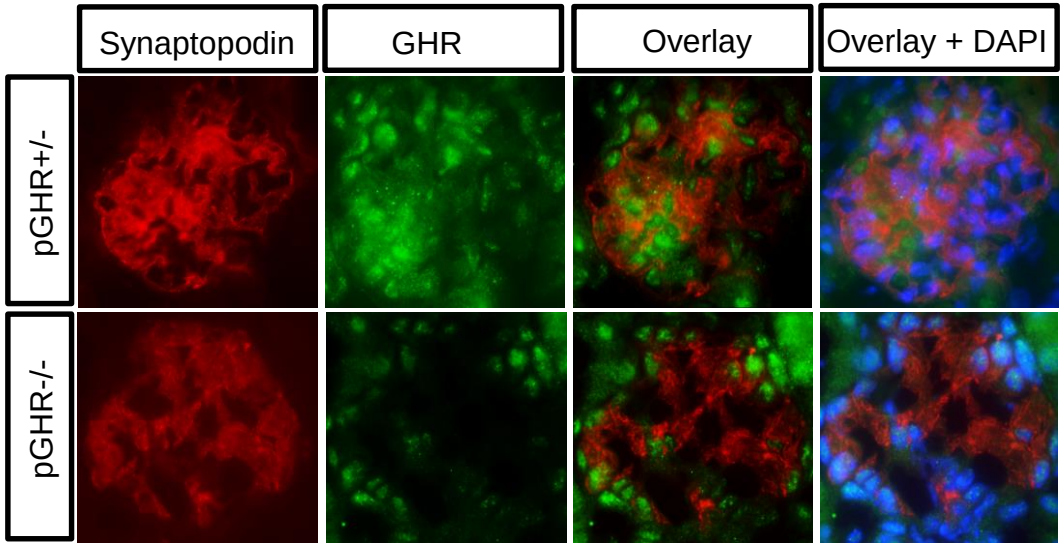
Synaptopodin
GHR
Overlay
Overlay + DAPI
pGHR+/-
pGHR-/-

B

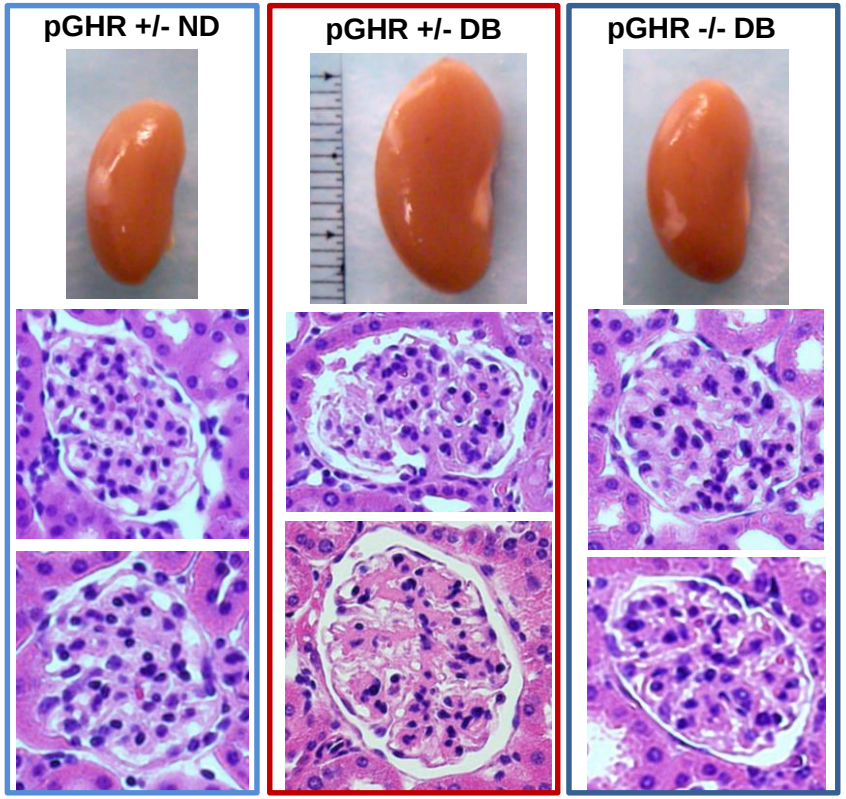
pGHR +/- ND
pGHR +/- DB
pGHR -/- DB

E

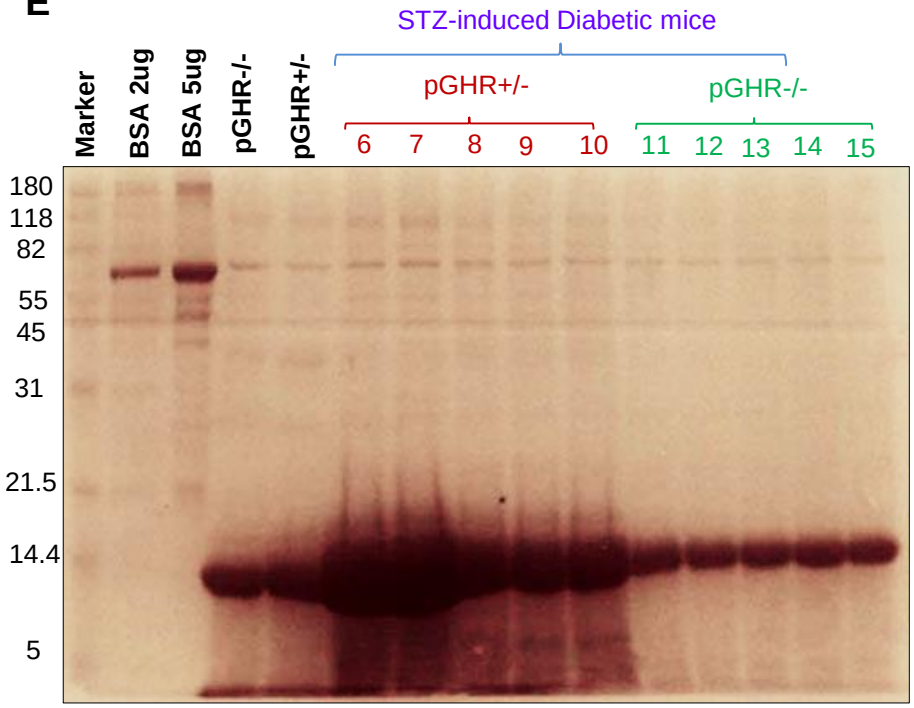
STZ-induced Diabetic mice
pGHR+/-
pGHR-/-
Marker
BSA 2ug
BSA 5ug
pGHR-/-
pGHR+/-
6
7
8
9
10
11
12
13
14
15
180
118
82
55
45
31
21.5
14.4
5

C

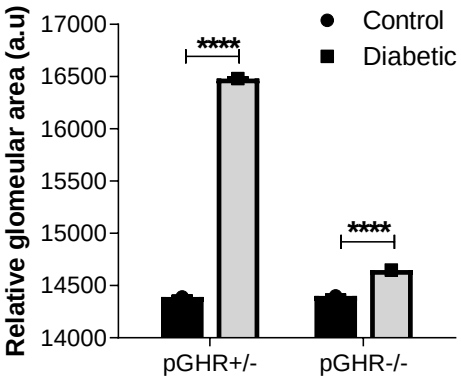
Relative glomeular area (a.u)
17000
16500
16000
15500
15000
14500
14000
****
****
Control
Diabetic
pGHR+/-
pGHR-/-

F

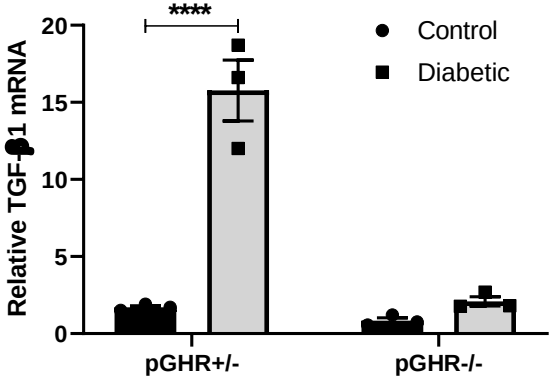
Relative TGF-β1 mRNA
20
15
10
5
0
****
Control
Diabetic
pGHR+/-
pGHR-/-

G

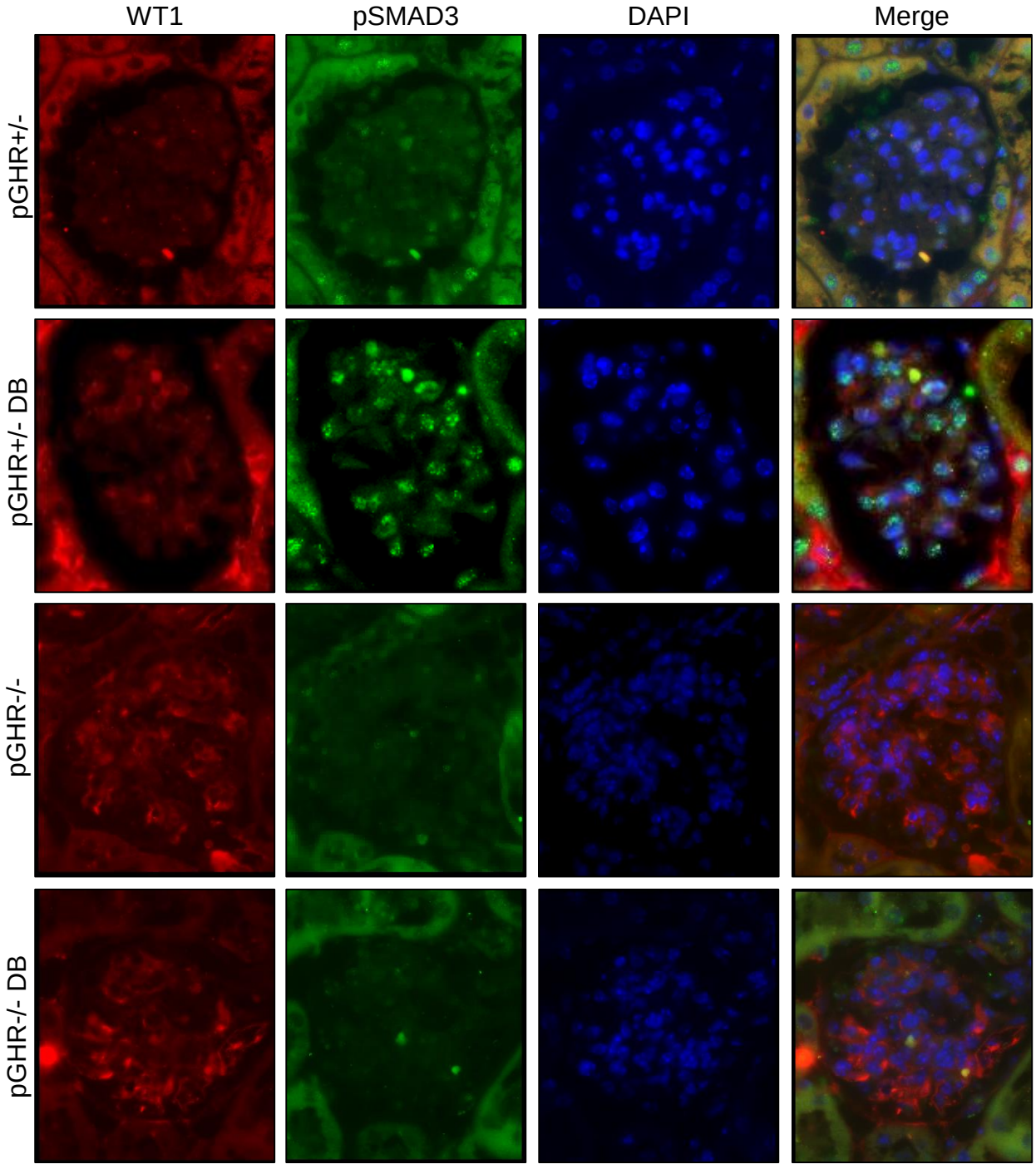
WT1
pSMAD3
DAPI
Merge
pGHR+/-
pGHR+/- DB
pGHR-/-
pGHR-/- DB

Table: List of parameters measured in animals

Parameter		Control	GH	GH+SB
Body weights (g)		33.4	33.7	33.7
Organ weights	Kidney (mg)	243.4	285.3	280
	Heart (mg)	182	207	189
	Lung (mg)	387.1	480	438.6
	Liver (g)	2.4	2.2	2.3
Fasting blood glucose (mg/dL)		124	151	159